



Shapley Value Method and Stochastic Dantzig–Wolfe Decomposition for Decentralized Scheduling of Multimicrogrid

Amit Singh , *Student Member, IEEE*, Basant Kumar Sethi , *Student Member, IEEE*, Devender Singh, and Rakesh Kumar Misra , *Member, IEEE*

Abstract—The decentralized economic scheduling of multimicrogrid is an important aspect in the operational planning of microgrids (MGs). This article proposes an approach to maximize economic benefit among MGs through cooperative scheduling. The cooperative scheduling is achieved via price signals so that MGs are encouraged to share power among themselves for economic benefit. An MG operator generates a time-variable tariff based on energy trading status so that the parking lot operator and distributed battery energy storage system aggregator participate with flexibility in the MG’s energy management. The Shapley value method is used for generating fair price signals. The stochastic Dantzig–Wolfe decomposition is used to solve the resulting optimization problem in a decentralized manner. The uncertainties related to load demand and renewable energy sources are captured using scenario-based methods, whereas the uncertainty associated with plug-in hybrid electric vehicles is modeled using copula theory based estimation. The simulation studies and comparison with the existing methods establish that the proposed approach effectively reduces the total energy cost in a decentralized manner with the minimum amount of information exchange.

Index Terms—Dantzig–Wolfe decomposition (DWD), distributed battery energy storage system (D-BESS), distributed generation (DG), multimicrogrid (MMG), plug-in hybrid electric vehicle (PHEV), Shapley value method (SVM).

NOMENCLATURE

η_c, η_d	Charging/discharging efficiency of charger.
$\lambda_{t,s}^m, \sigma_{PL}, \sigma_{BESS}$	Dual variables.
$\overline{P}_{t,s}^{MT}$	Maximum available capacity of MT at time t under scenario s (p.u.).
ϕ_t^k	Profit/loss allocated to k th MG at time t (€).
π_s	Probability of scenario s .
$\psi_t(S)$	Profit/loss of coalition S at time t (€).
$\psi_t(S - \{k\})$	Profit/loss of coalition S , without participation of the k th MG at time t (€).
ρ^{emi}	Emission tariff (€ /kWh).
ρ_t^c, ρ_t^d	Charge/discharge tariff of MG (€ /kWh).
$\rho_t^{c,DU}, \rho_t^{d,DU}$	Import/export tariff of DU (€ /kWh).
ρ_t^{cur}	RES curtailment price (€ /kWh).

Manuscript received November 1, 2020; revised April 27, 2021 and August 30, 2021; accepted October 6, 2021. Date of publication November 18, 2021; date of current version June 13, 2022. (*Corresponding author: Amit Singh.*)

The authors are with the Department of Electrical Engineering, Indian Institute of Technology (BHU) Varanasi, Varanasi 221005, India (e-mail: amitsingh.rs.eee17@iitbhu.ac.in).

Digital Object Identifier 10.1109/JSYST.2021.3119426

$\rho_t^{\text{im},k}, \rho_t^{\text{ex},k}$	Import/export tariff for k th MG (€ /kWh).
$\rho_t^{\text{up}}, \rho_t^{\text{do}}$	Up/down-SR tariff (€ /kWh).
$\frac{\Delta P, \overline{\Delta P}}{P, \overline{P}}$	Minimum/maximum limit of load shift (p.u.).
BC	Minimum/maximum limit of net power from PLs and D-BESSs (p.u.).
$C_{t,s}^{\text{MT}}, C_{t,s}^{\text{SR}}$	Battery capacity (p.u.).
$E_{t,t'}$	Cost of MT/spinning reserve at time t under scenario s (€).
$N_s, N_{\text{ev}}, N_{\text{bess}}$	Load elasticity coefficient.
$P_{\text{max}}^c, P_{\text{max}}^d$	Total number of scenarios, PHEVs in PL, and D-BESSs, respectively.
$P_{\text{max}}^{\text{im},k}, P_{\text{max}}^{\text{ex},k}$	Rated charging/discharging capacity of battery (p.u.).
$P_{\text{max}}^{\text{MT}}, P_{\text{min}}^{\text{MT}}$	Maximum limit of power import/export for k th MG (p.u.).
$P_{t,s}^{c,b}, P_{t,s}^{d,b}$	MT maximum/minimum power limit (p.u.).
$P_{t,s}^{c,ev}, P_{t,s}^{d,ev}$	Charging/discharging power of D-BESS at time t under scenario s (p.u.).
$P_{t,s}^{\text{cur}}$	Charging/discharging power of PHEV at time t under scenario s (p.u.).
$P_{t,s}^{\text{im},k}, P_{t,s}^{\text{ex},k}$	Expected RES curtailed power at time t under scenario s (p.u.).
$P_{t,s}^{\text{in,PL}}, P_{t,s}^{\text{out,PL}}$	k th MG import/export power at time t under scenario s (p.u.).
$P_{t,s}^{\text{PL}}, P_{t,s}^{\text{SL}}$	Power import/export by parking lot at time t under scenario s (p.u.).
$P_{t,s}^{\text{MT}}, \text{RD}^{\text{MT}}$	Elastic load before/after load shifting at time t under scenario s (p.u.).
$S_{t,s}^{\text{up},b}, S_{t,s}^{\text{do},b}$	MT power at time t under scenario s (p.u.).
$S_{t,s}^{\text{up,MT}}, S_{t,s}^{\text{do,MT}}$	Ramp-up/down limit of MT.
$\text{SOC}_{\text{max}/\text{min}}, \text{SOC}_{t,s}$	D-BESS contribution in up/down-SR (p.u.).
$\text{SU}^{\text{MT}}, \text{SD}^{\text{MT}}$	MT contribution in up/down-SR (p.u.).
$t_{\text{arri}}, t_{\text{depa}}$	Maximum/minimum SOC limit (%).
$u_w^{\text{PL}}, u_w^{\text{BESS}}$	State of charge (SOC) at time t under scenario s (%).
$u_{t,s}^{\text{exc},k}$	Startup/shutdown ramp limit of MT.
	Index for time, scenario, D-BESS, PHEV, and MG, respectively.
	Arrival/departure time of PHEV.
	Weight factor for the w th proposal.
	Battery charging status.
	k th MG power import/export status at time t under scenario s .

$u_{t,s}^{\text{MT}}$	MT ON/OFF status at time t under scenario s .
w	Proposal index in SDWD.
$Z_{\omega,s}^{\text{PL}}, Z_{\omega,s}^{\text{BESS}}$	Energy cost of PL operator/D-BESS aggregator for the w th proposal.

I. INTRODUCTION

IN THE present active distribution system, diverse resources, namely, plug-in hybrid electric vehicles (PHEVs), battery energy storage systems (BESSs), and renewable energy sources (RESs), play vital role in energy management. Contrary to the benefits of PHEVs and RES, such as real power loss reduction, low carbon emissions, demand curve flattening, etc., they also pose some challenges to the distribution system. The intermittent nature of RES increases uncertainty on the supply side, whereas the uncontrolled charging/discharging of PHEVs increase uncertainty on the demand side.

In recent years, many studies have focused on coordinated optimal scheduling of diverse energy resources to achieve various objectives, such as peak shaving, energy cost minimization, voltage profile improvement, ancillary services deployment, power loss minimization, and greenhouse gas emission reduction, [1]–[4]. The term peak shaving is related to reducing the power consumption during peak demand periods. This may be achieved by load shedding or by activating distributed energy resources. The BESS plays an important role to accommodate high penetration of RES. The BESS is capable of reducing energy procurement costs, reducing power losses, and improving reliability [5]. Large battery capacities of PHEVs enable them to be used for energy storage during their parking time. In smart parking lots (PLs), battery storage of electric vehicles (EVs) can support microgrid (MG) by realizing the grid-to-vehicle and vehicle-to-grid concept considering owner's satisfaction parameters [6]–[8]. The PHEVs as energy storage have been used for peak shaving and mitigating the effects of RES variability in the distribution system as reported in [9]–[12].

A. Literature Review

Multimicrogrid (MMG) energy management has been investigated in the literature. Some researchers have used central controllers for MGs, whereas some researchers have considered MG operators (MGOs) as separate bodies to optimize their assets independently. Competitive as well as collaborative strategies based on intermediate platforms have been investigated for trading power between MG and distribution utility (DU). A non-pricing trading mechanism has been proposed in [13]. In [13], the allocation of the surplus energy of seller MGs to buyer MGs is based on the priority index. A decentralized bilevel model has been used to trade power between MGs and distribution network operator (DNO) in a networked MMG system in [14]. Each of the MGs and DNO has been considered as independent entity with the objective of minimizing its operating cost. Although MGs and DNO have a coordinated operation, no mechanism has been proposed in [14] that encourages MGOs to prefer interchange power among themselves instead of DNO. A power-sharing optimization problem to minimize energy cost for grid-connected MMG system has been introduced in [15]. The MGs are classified into priority groups according to their RES and storage capacity, and treated with lexicographic programming.

This model demands large flow of bidirectional information between the central controller and MGs, i.e., net demand of all MGs, energy levels of storage units, and commands from the central controller to local controllers. Also, the power exchange prices between MGs are prefixed based on grid prices. Y. Wang *et al.* [16] have developed a two-tier optimization problem for managing storage and power exchange between MG and grid. User utility function, power transmission cost, and load variance optimization have been considered in first-tier, whereas the generation and transmission cost for MGs has been dealt with in the second-tier. A centralized energy management system (EMS) for grid-connected MMG system has been discussed in [17]. In [17], a common control center has been used to optimize all MGs' assets. No mechanism has been depicted to promote MGOs to change their net power demand according to the demand of other MGs. A cooperative model predictive control based EMS for minimizing power exchange with the grid and local level generation cost has been developed in [18]. In order to coordinate all MGs, an optimization phase considering guaranteed benefit for all MGs has been included between the initial and final optimization phase at individual MG level. A day-ahead coordinated energy scheduling to minimize the energy cost of the MMG system, consisting of dispatchable/nondispatchable distributed generation (DG), energy storage, and EVs, has been investigated in [19]. A central operator controls all the generation and consumption unit of MGs. A novel cooperative game theory based coalitional economic dispatch problem has been formulated for a distribution system containing MMG [20]. Another type of cooperative energy management framework aiming at operation cost minimization and power exchange from grid minimization has been studied in [21]. Pricing model for power exchange among MGs has not been discussed in this multiobjective centrally optimized framework. In [22], a bilevel model for energy management of MMG has been proposed. The outer level takes care of power-sharing during the networked operation of MG, and the inner level takes care of energy management of isolated MG. A weighted average of marginal prices of the seller and buyer MGs has been used as a price for power exchange between MGs. A Nash bargaining theory based incentive mechanism for power trading between MGs has been proposed in [23]. This article uses an alternating direction method of multipliers based decentralized approach for scheduling and trading benefit sharing. A comparison-based analysis of cooperative and noncooperative game theory based optimization of BESS in the MMG system proposed in [24] illustrated that the cooperative operation provides lower daily operating cost.

B. Motivation

The aforementioned studies show the advantages of coordinated operation of MMG. Each MGO aims to achieve economic benefits by utilizing energy resources in its entity. In the non-interactive approach, they optimize their assets and exchange power with DU according to consumers' demand response (DR), generation availability, and energy tariff of the upstream grid. In cooperative operation, MGs exchange power among themselves for more benefits. Here, in cooperative operation, instead of DNO, MGOs exchange power among themselves as

much as possible. Each MG may have distinct surplus/deficit energy periods due to nonidentical consumer demand pattern and generation availability. They can exchange power among themselves at a settled price for economic profit rather than the price set by the DNO.

In the existing literature, the coupling constraints are used between the MGs for economic benefit based power exchange. A joint scheduling of all MGs is required to deal with these coupling constraints. One of the important research gaps in the present scenario is that a dedicated communication network between all MGOs, and MGOs and DNO, is mandatory to exchange information in both centralized or decentralized approaches. This also amounts to increase in the complexity of the communication network with increase in number of MGOs. For example, in the case of (n) networked MGs system, each MGO is required to communicate with DNO and $(n - 1)$ MGOs to select the best pairs to exchange power. Besides the communication requirements, sharing of information/data of MGs is also assumed, which may be sensitive hence may not be shareable.

C. Contribution

This article proposes a novel decentralized EMS for networked MMG to optimize MGO-owned energy resources and prosumers with minimum mandatory information sharing. In the proposed method, the pricing signal is used to coordinate all MGOs and encourage them to exchange power among themselves for economic benefits. The power exchange unlike present approaches does not require any coupling constraint between MGOs, thereby eliminating the mandatory need for information exchange between MGOs, and the joint scheduling of all MGs for cooperative operations. Each MGO is only required to submit its power exchange request to an external agent called MGs' aggregator (MGA). The MGA communicates a new price signal for each MGO, subject to the contributions to the energy pool of the MGOs. The Shapley value method (SVM) is used to update the price signal for each MGO fairly. All MGOs can reschedule their assets independently based on the updated price.

Additionally, the PLs and distributed battery energy storage systems (D-BESSs) are considered as profit-based entities. Scenarios based on historical data are used to deal with uncertainties related to load demand and RES, whereas uncertainties associated with PHEV are captured with copula theory based estimation of driving behavioral parameters. The above said contributions of this article are achieved in the following manner.

- 1) An SVM-based framework is developed for the cooperative operation of MGs to reduce the operating cost. The SVM is used to fairly allocate profit/cost hourly at the MGA level, which is used to determine the updated electricity tariff for individual MGO.
- 2) A stochastic Dantzig–Wolfe decomposition (SDWD) approach for decentralized scheduling of MGs and their prosumers, i.e., PLs and D-BESSs.
- 3) MGO's trading status based time-variable tariffs are used to emphasize the flexibility and contribution of PLs and D-BESSs in MG's energy management.

The rest of this article is organized as follows. Section II summarizes the system model and basic architecture of EMS. Section III describes the problem formulation. The methodology

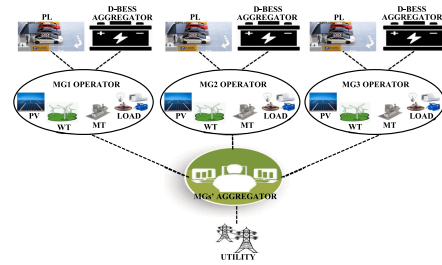


Fig. 1. Conceptual diagram of MMG energy management framework.

and process flow are described in Section IV. Section V details out the findings to demonstrate the effectiveness of the proposed formulation. Finally, Section VI concludes this article.

II. SYSTEM MODEL

In this article, the energy management of MMG is considered with energy cost minimization objective. Each MG consists of microturbines (MTs), RES, i.e., wind turbines and photovoltaics (PVs) [25], prosumers (PLs and D-BESSs), and consumer loads. The different components of the framework and their communication links are illustrated in Fig. 1. All the MGs can trade power among themselves or with DU. The PL and D-BESS are self-governed entities, but they have to follow some constraints or presigned agreements, such as the maximum limit of power demand, etc. MGO offers electricity tariff to PL and D-BESS, they respond back with their demands to MGO. Each MGO receives electricity tariff from MGA and independently schedules its energy resources to satisfy the demand from PLs, D-BESSs, and conventional users. After that, MGO sends a power exchange request to MGA. On the basis of each MG participation, MGA allocates power transfer from MG to MG or MG to DU and updates electricity prices for each MG. The detail description of this framework is given in Section IV.

A. Stochastic Model of PL

The power exchange capability, i.e., PL to grid (PL2G) and grid to PL (G2PL), of PLs depends on their customers' driving habits and the type of their vehicles. Arrival time, departure time, and daily driven miles are driving habit related parameters, whereas the battery capacities and rated charging/discharging power depend on the type of vehicles. In this work, the National Household Travel Survey (NHTS) 2017 database [26] is used to model the stochastic driving pattern. The NHTS 2017 database contains 129 112 household surveys. We consider the first trip end time as the arrival time of PHEV in PLs and the next trip start time as the departure time of PHEV from PLs. According to NHTS 2017 database, the arrival time, departure time, and miles driven by PHEVs can be described by generalized extreme value distribution $GEV(0.0693, 8.528, 2.479)$, $GEV(-0.491, 15.551, 4.025)$ and lognormal distribution $Lognormal(3.142, 1.0271)$, respectively. The probability density function (pdf) of $GEV(\kappa, \mu, \varsigma)$ distribution of arrival and departure time of PHEVs can be described

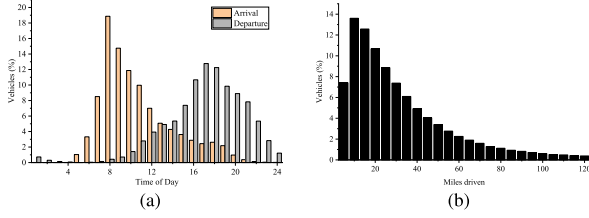


Fig. 2. Histogram of (a) arrival and departure times and (b) daily miles driven by PHEVs.

as

$$pdf = \begin{cases} \left(\frac{1}{\zeta}\right) \left(1 + \kappa \frac{(t-\mu)}{\zeta}\right)^{-\frac{(\kappa+1)}{\kappa}} e^{-(1+\kappa \frac{(t-\mu)}{\zeta})^{-\frac{1}{\kappa}}}, & \kappa \neq 0 \\ \left(\frac{1}{\zeta}\right) e^{-\left(\frac{(t-\mu)}{\zeta} + e^{-\frac{(t-\mu)}{\zeta}}\right)}, & \kappa = 0 \end{cases}$$

where κ , μ , and ζ are the shape, location, and scale parameters, respectively.

Similarly, the pdf of Lognormal($\bar{\mu}$, $\bar{\zeta}^2$) distribution of daily miles driven by PHEVs can be expressed as

$$pdf = \frac{1}{\Gamma \bar{\zeta} \sqrt{2\pi}} e^{-\frac{(\ln \Gamma - \bar{\mu})^2}{2\bar{\zeta}^2}}$$

where $\bar{\zeta}$ and $\bar{\mu}$ are the standard deviation and mean of $\ln \Gamma$, respectively. Γ represents the miles driven by PHEVs.

Histograms of arrival time, departure time, and driven miles are shown in Fig. 2. As depicted in Fig. 2(a), the arrival time of about 70% PHEVs is between 7:00–12:00 h, whereas the departure time of about 70% PHEVs is between 15:00–21:00 h. Each bar in Fig. 2(b) represents the PHEVs' percentage with a particular mileage range. Approximately 70% PHEVs drive less than 40 mi/d.

The rank correlation between arrival time, departure time, and daily driven miles is shown in (1), verifying the monotonic dependence of these three parameters

$$\tau = \begin{bmatrix} 1 & 0.0761 & -0.1029 \\ 0.0761 & 1 & 0.1334 \\ -0.1029 & 0.1334 & 1 \end{bmatrix}. \quad (1)$$

A copula function can be employed to find the joint distribution function of these three statistically dependent parameters with different marginal distribution. A copula function joins the univariate marginal distribution of multiple random variables to form the multivariate distribution function. For modeling the driving behavior of PHEVs' users, the Gaussian copula is used in this article. The detailed procedure for simulating dependent random parameters using copula can be found in [27]. It is to be noted that these three parameters are used to estimate the energy exchange pattern of PLs for the next day. The real-time arrival/departure time of PHEVs may differ, but the copula theory based simulated parameters can forecast the cumulative demand pattern of all PHEVs in PLs. Based on simulated miles driven data, the initial battery status of PHEV, $\text{SOC}_{t_{\text{arri}}}^{ev}$ can be calculated as

$$\text{SOC}_{t_{\text{arri}}}^{ev} = \begin{cases} \left(1 - \frac{\Gamma \Upsilon}{\Gamma_{\text{aer}}}\right) 100, & \Gamma \Upsilon \leq \Gamma_{\text{aer}} \\ 0, & \Gamma \Upsilon \geq \Gamma_{\text{aer}} \end{cases}$$

where, Γ , Υ , and Γ_{aer} represent the miles driven by PHEV, the fraction of miles driven in electric mode, and the all-electric range of PHEV, respectively.

III. PROBLEM FORMULATION

A. Energy Cost Minimization

The goal of this article is to minimize the operating cost of MG (f_{MG}), PLs (f_{PL}), and D-BESSs ($f_{\text{D-BESS}}$). The energy cost minimization function (F) can be defined as

$$\min F = f_{\text{MG}} + f_{\text{PL}} + f_{\text{D-BESS}}. \quad (2)$$

All the three components of the energy cost function F are subjected to some distinctive and coupling constraints. The uncertainties related to RES power and consumer loads are simulated through Monte Carlo simulation (MCS) based scenarios. MCS is used to generate a large number of samples of RES generation and consumer loads. It is a very time-consuming process to simulate the scheduling algorithm with such a large number of samples. The scenario reduction algorithm [28] is used to reduce the number of scenarios generated in MCS to an appropriate number to reduce computational complexity. The components f_{MG} , f_{PL} , and $f_{\text{D-BESS}}$ with their constraints are described in the following section.

B. PLs and Distributed Battery Energy Storage Objective

The purpose of the PL operator is to reduce the operating cost of the PL under the tariff structure by the MGO with the satisfaction of the owner of the PHEVs. It is assumed that the PLs are equipped with both PL2G and G2PL facility. The operating cost of PLs can be defined as the difference between the cost of electric energy purchase in G2PL mode and the income from electric energy feed back to MG in PL2G mode. Thus, f_{PL} can be expressed as

$$f_{\text{PL}} = \sum_{s=1}^{N_s} \pi_s \sum_{t=1}^T (P_{t,s}^{\text{in,PL}} \rho_t^c - P_{t,s}^{\text{out,PL}} \rho_t^d) \quad (3)$$

where π_s is the probability of scenario s . The G2PL power $P_{t,s}^{\text{in,PL}}$ and PL2G power $P_{t,s}^{\text{out,PL}}$ can be defined as

$$P_{t,s}^{\text{in,PL}} = \max\left(0, \sum_{ev=1}^{N_{ev}} (P_{t,s}^{c,ev} - P_{t,s}^{d,ev})\right)$$

$$P_{t,s}^{\text{out,PL}} = \max\left(0, \sum_{ev=1}^{N_{ev}} (P_{t,s}^{d,ev} - P_{t,s}^{c,ev})\right).$$

The D-BESS aggregator stores energy during a low tariff period and feeds back to MG during a high tariff period. The objective of the D-BESS aggregator is to maximize their profit ($-f_{\text{D-BESS}}$). The component related to D-BESSs $f_{\text{D-BESS}}$ in the cost function F can be described as

$$f_{\text{D-BESS}} = \sum_{s=1}^{N_s} \pi_s \sum_{t=1}^T \sum_{b=1}^{N_b} (P_{t,s}^{c,b} \rho_t^c - P_{t,s}^{d,b} \rho_t^d) \quad (4)$$

where $P_{t,s}^{c,b}$ and $P_{t,s}^{d,b}$ denote the charging and discharging power of D-BESS, respectively.

Both PHEVs and D-BESSs are subjected to following constraints:

$$P_{t,s}^c \leq u_{t,s} P_{\max}^c \quad (5)$$

$$P_{t,s}^d \leq (1 - u_{t,s}) P_{\max}^d \quad (6)$$

$$\text{SOC}_{t,s} = \text{SOC}_{t-1,s} + \frac{100}{\text{BC}} \left(\eta_c P_{t,s}^c - \frac{P_{t,s}^d}{\eta_d} \right) \quad (7)$$

$$\text{SOC}_{\min} \leq \text{SOC}_{t,s} \leq \text{SOC}_{\max} \quad (8)$$

$$\text{SOC}_{t_{\text{depa}},s}^{\text{ev}} = \min \left[\text{SOC}_{\max}, \left(\text{SOC}_{t_{\text{arri}}}^{\text{ev}} + \frac{100 \times \eta_c P_{\max}^{\text{c,ev}} \Delta T}{\text{BC}^{\text{ev}}} \right) \right] \quad (9)$$

$$\sum_{t=1}^T \eta_c P_{t,s}^{\text{c,b}} = \sum_{t=1}^T \frac{P_{t,s}^{\text{d,b}}}{\eta_d} \quad (10)$$

$$\underline{P} \leq (P_{t,s}^{\text{in,PL}} - P_{t,s}^{\text{out,PL}}) + \sum_{b=1}^{N_b} (P_{t,s}^{\text{c,b}} - P_{t,s}^{\text{d,b}}) \leq \bar{P}. \quad (11)$$

According to battery charger specifications, (5) and (6) impose the bound on charging and discharging power. These two constraints also prohibit the simultaneous charging and discharging of a battery. Binary variable $u_{t,s}$ indicates the charging/discharging status of the battery, 1 for charging and 0 for discharging. The next stage state of charge (SOC) $\text{SOC}_{t,s}$ of a PHEV or a D-BESS depends on present SOC and charging/discharging status, and this relation can be defined as (7). The battery SOC is subjected to maximum and minimum limits (8). The constraint (9) ensures the maximum possible SOC at the time of departure of PHEV. This constraint is related to PHEV owner satisfaction, and SOC_{\max} can be replaced with PHEV owner's desired SOC level. The constraint (10) makes sure that the D-BESSs' net storage used is equal to zero over a day. This constraint is required for next-day availability of D-BESS and continuity in scheduling. The net power demand/supply of PLs and D-BESSs is restricted to maximum and minimum limits by MGO (11). This constraint requires coordination between both the prosumers.

C. MG Objective

The MGO schedules its assets and exchanges power with the other MGs and DU to satisfy the consumers' (and prosumers') demand of its entity. The MGO aims to minimize the MTs' operating cost, power import cost, spinning reserves' (SRs) cost, and emission cost while maximizing the power export cost. Thus, the objective function for k th MGO can be written as

$$f_{\text{MG}} = \sum_{s=1}^{N_s} \pi_s \sum_{t=1}^T (C_{t,s}^{\text{MT}} + P_{t,s}^{\text{im},k} \rho_t^{\text{im},k} - P_{t,s}^{\text{ex},k} \rho_t^{\text{ex},k} + C_{t,s}^{\text{SR}} + P_{t,s}^{\text{MT}} \rho_t^{\text{emi}}) \quad (12)$$

where import and export powers of MG are denoted by $P_{t,s}^{\text{im},k}$ and $P_{t,s}^{\text{ex},k}$, respectively. MTs' generation cost $C_{t,s}^{\text{MT}}$ and SR cost $C_{t,s}^{\text{SR}}$ can be defined as

$$C_{t,s}^{\text{MT}} = \beta^{\text{MT}} P_{t,s}^{\text{MT}} + \gamma^{\text{MT}} (P_{t,s}^{\text{MT}})^2$$

$$C_{t,s}^{\text{SR}} = (S_{t,s}^{\text{up,MT}} + S_{t,s}^{\text{up,b}}) \rho_t^{\text{up}} + (S_{t,s}^{\text{do,MT}} + S_{t,s}^{\text{do,b}}) \rho_t^{\text{do}} + P_{t,s}^{\text{cur}} \rho_t^{\text{cur}}.$$

The cost function of MT $C_{t,s}^{\text{MT}}$ can be linearized by using a piecewise linear function [29]. The SR cost of MG includes the D-BESSs' and MTs' SR cost, and the expected RES curtailment cost in case of insufficient down-SR.

The MGO problem is subjected to some constraints, i.e., MT operating limits, RES power availability, power exchange bounds, consumers load elasticity limits, SRs requirement, and load balancing. These constraints can be described as follows:

$$P_{t,s}^{\text{im},k} \leq u_{t,s}^{\text{exc},k} P_{\max}^{\text{im},k} \quad (13)$$

$$P_{t,s}^{\text{ex},k} \leq (1 - u_{t,s}^{\text{exc},k}) P_{\max}^{\text{ex},k} \quad (14)$$

$$u_{t,s}^{\text{MT}} P_{\min}^{\text{MT}} \leq P_{t,s}^{\text{MT}} \leq \overline{P_{t,s}^{\text{MT}}} \quad (15)$$

$$0 \leq \overline{P_{t,s}^{\text{MT}}} \leq u_{t,s}^{\text{MT}} P_{\max}^{\text{MT}} \quad (16)$$

$$\overline{P_{t,s}^{\text{MT}}} - P_{t-1,s}^{\text{MT}} \leq u_{t-1,s}^{\text{MT}} \text{RU}^{\text{MT}} + (u_{t,s}^{\text{MT}} - u_{t-1,s}^{\text{MT}}) \text{SU}^{\text{MT}} + (1 - u_{t,s}^{\text{MT}}) P_{\max}^{\text{MT}} \quad (17)$$

$$P_{t-1,s}^{\text{MT}} - P_{t,s}^{\text{MT}} \leq u_{t,s}^{\text{MT}} \text{RD}^{\text{MT}} + (u_{t-1,s}^{\text{MT}} - u_{t,s}^{\text{MT}}) \text{SD}^{\text{MT}} + (1 - u_{t-1,s}^{\text{MT}}) P_{\max}^{\text{MT}} \quad (18)$$

$$\overline{P_{t,s}^{\text{MT}}} \leq u_{t+1,s}^{\text{MT}} P_{\max}^{\text{MT}} + (u_{t,s}^{\text{MT}} - u_{t+1,s}^{\text{MT}}) \text{SU}^{\text{MT}} \quad (19)$$

$$P_{t,s}^{\text{SL}} = P_{t,s}^L \left[1 + \sum_{t'=1}^T E_{t,t'} \left(\frac{\rho_{t',s}^{\text{new}} - \rho_{t'}^{\text{v}}}{\rho_{t'}} \right) \right] \quad (20)$$

$$\underline{\Delta P} \leq (P_{t,s}^{\text{SL}} - P_{t,s}^L) \leq \overline{\Delta P} \quad (21)$$

$$\sum_{t=1}^T (P_{t,s}^{\text{SL}} - P_{t,s}^L) = 0 \quad (22)$$

$$P_{t,s}^{\text{im},k} + P_{t,s}^{\text{MT}} + P_{t,s}^W + P_{t,s}^{\text{PV}} - P_{t,s}^{\text{ex},k} - P_{t,s}^{\text{SL}} - P_{t,s}^{\text{in,PL}} + P_{t,s}^{\text{out,PL}} - \sum_{b=1}^{N_b} (P_{t,s}^{\text{c,b}} - P_{t,s}^{\text{d,b}}) = 0 \quad (23)$$

$$S_{t,s}^{\text{up,MT}} \leq \min((\overline{P_{t,s}^{\text{MT}}} - P_{t,s}^{\text{MT}}), u_{t,s}^{\text{MT}} \text{RU}^{\text{MT}}) \quad (24)$$

$$S_{t,s}^{\text{do,MT}} \leq \min((P_{t,s}^{\text{MT}} - u_{t,s}^{\text{MT}} P_{\min}^{\text{MT}}), u_{t,s}^{\text{MT}} \text{RD}^{\text{MT}}) \quad (25)$$

$$S_{t,s}^{\text{up,b}} \leq \min((P_{\max}^d - P_{t,s}^{\text{d,b}} + P_{t,s}^{\text{c,b}}) (0.01 \eta_d \text{BC} (\text{SOC}_{t,s}^b - \text{SOC}_{\min}))) \quad (26)$$

$$S_{t,s}^{\text{do,b}} \leq \min((P_{\max}^c - P_{t,s}^{\text{c,b}} + P_{t,s}^{\text{d,b}}) (\frac{0.01 \text{BC}}{\eta_c} (\text{SOC}_{\max} - \text{SOC}_{t,s}^b))) \quad (27)$$

$$P_{t,s}^W - P_{t,\min}^W + P_{t,s}^{\text{PV}} - P_{t,\min}^{\text{PV}} - S_{t,s}^{\text{up,MT}} - \sum_{b=1}^{N_b} S_{t,s}^{\text{up,b}} \leq 0 \quad (28)$$

$$P_{t,\max}^W - P_{t,s}^W + P_{t,\max}^{\text{PV}} - P_{t,s}^{\text{PV}} - S_{t,s}^{\text{do,MT}} - \sum_{b=1}^{N_b} S_{t,s}^{\text{do,b}} - P_{t,s}^{\text{cur}} \leq 0. \quad (29)$$

The maximum power import/export limits are bounded by constraints (13) and (14). Also, these two constraints prohibit simultaneous power import and export. Binary variable $u_{t,s}^{\text{exc},k}$ represents the import/export status of MG, 1 for import and 0 for export the power. Constraints (15) and (16) limit the MT power generation $P_{t,s}^{\text{MT}}$. Ramp-up and ramp-down limits are imposed by (17)–(19) [29]. $\text{RU}^{\text{MT}}/\text{RD}^{\text{MT}}$ are the ramp-up/down limits, whereas $\text{SU}^{\text{MT}}/\text{SD}^{\text{MT}}$ are the startup/shutdown ramp limits of MT. Time of use based DR is modeled by using the price elasticity of demand [30]. Before and after load-shifting, the elastic load is represented by $P_{t,s}^{\text{L}}$ and $P_{t,s}^{\text{SL}}$, respectively. A linear response function of price elasticity (20) is used to obtain the modified demand. Equation (21) bounds the load shift in the DR program to an allowable limit. Constraint (22) indicates that there is no load curtailment in the DR program, i.e., consumer load can be shifted from one time period to another time period. Load balancing constraint (23) is a coupling constraint for MG, PLs, and D-BESSs.

The up-SR availability of MT (24) is subjected to scheduled output power $P_{t,s}^{\text{MT}}$ and maximum available capacity $\overline{P}_{t,s}^{\text{MT}}$ at that time. It must also satisfy the ramp-up limit of the generator. Similarly, the down-SR capability (25) depends on the ramp-down limit, and the difference between $P_{t,s}^{\text{MT}}$ and the lower limit of MT. The D-BESS contribution in SR depends on present SOC, charging/discharging state, and maximum power limits. The up-SR (or down-SR) of D-BESS can be defined as maximum effective power injection (or absorbing) capability of D-BESS into/from the MG at that instant. The up- and down-SR are calculated using (26) and (27), respectively. The minimum up/down-SR requirement for reliable operation to manage the uncertainty of RES can be defined by (28) and (29). In this article, we consider that the up-SR should be greater than the difference between total energy harvested from RES ($P_{t,s}^{\text{W}} + P_{t,s}^{\text{PV}}$) and minimum expected RES power ($P_{t,\min}^{\text{W}} + P_{t,\min}^{\text{PV}}$) in all scenarios in that interval. The down-SR should be greater than the difference between the maximum expected RES power ($P_{t,\max}^{\text{W}} + P_{t,\max}^{\text{PV}}$) and total energy harvested from RES.

IV. METHODOLOGY

A. Stochastic Dantzig–Wolfe Decomposition

The PL operator, D-BESS aggregator, and MGO need a coordinated operation to satisfy coupling constraints. But they may be concerned about their privacy and want to share the minimum possible information for coordination. A decentralized technique is required to tackle this optimization problem. A decentralized approach, the Dantzig–Wolfe decomposition (DWD) method [31], can be used to find the optimal global solution of a linear optimization problem with some coupling constraints. The problem described in Section III can be optimized in a decentralized manner by using SDWD. The constraints (11), (23), (28), and (29) are coupling constraints, as these four constraints contain variables related to two or more operators, i.e., PL operator, D-BESS aggregator, and MGO. The original optimization problem can be restructured as two subproblems (related to PL operator and D-BESS aggregator) and one master problem. All coupling constraints and MGO related constraints are associated with the master problem. The dual variables from

the master problem are used to penalize the subproblems. So, the PL operator and D-BESS aggregator manage their scheduling according to these dual variables and energy tariff provided by MGO. They only need to share their net electricity demand proposals with MGO rather than personal data of individual consumers, such as arrival time, departure time, and battery energy level, etc. The detailed mathematical reformulation can be described as master problem and subproblems in the following manner.

The master problem

$$\begin{aligned} \min \sum_{s=1}^{N_s} \pi_s \sum_{t=1}^T & \left[(C_{t,s}^{\text{MT}} + P_{t,s}^{\text{im},k} \rho_t^{\text{im},k} - P_{t,s}^{\text{ex},k} \rho_t^{\text{ex},k}) \right. \\ & + S_{t,s}^{\text{up,MT}} \rho_t^{\text{up}} + S_{t,s}^{\text{do,MT}} \rho_t^{\text{do}} + P_{t,s}^{\text{cur}} \rho_t^{\text{cur}} + P_{t,s}^{\text{MT}} \rho_t^{\text{emi}} \\ & \left. + \sum_{\omega} (Z_{\omega,s}^{\text{PL}} u_{\omega}^{\text{PL}} + Z_{\omega,s}^{\text{BESS}} u_{\omega}^{\text{BESS}}) \right] + \sum_{t=1}^T \text{pen}_t \end{aligned} \quad (30)$$

where $Z_{\omega,s}^{\text{PL}}$ and $Z_{\omega,s}^{\text{BESS}}$ are cost related to PL and D-BESS for ω th proposal. The decision variables u_{ω}^{PL} and u_{ω}^{BESS} assign weights to the PL operator and D-BESS aggregator proposals. $Z_{\omega,s}^{\text{PL}}$ and $Z_{\omega,s}^{\text{BESS}}$ can be defined as

$$Z_{\omega,s}^{\text{PL}} = \sum_{t=1}^T (P_{\omega,t,s}^{\text{in,PL}} \rho_t^c - P_{\omega,t,s}^{\text{out,PL}} \rho_t^d) \quad (31)$$

$$Z_{\omega,s}^{\text{BESS}} = \sum_{t=1}^T \sum_{b=1}^{N_b} (P_{\omega,t,s}^{c,b} \rho_t^c - P_{\omega,t,s}^{d,b} \rho_t^d + S_{\omega,t,s}^{\text{do},b} \rho_t^{\text{do}} + S_{\omega,t,s}^{\text{up},b} \rho_t^{\text{up}}). \quad (32)$$

A factor $\sum_{t=1}^T \text{pen}_t$ is used to force the MGO to minimize the changes in hourly net power demand in two consecutive iterations. K increase linearly as the iteration count increases

$$\text{pen}_t = K \left(\left| \sum_{s=1}^{N_s} \pi_s P_{t,s}^{\text{im},k} - P_{t,\text{iter}-1}^{\text{im},k} \right| + \left| \sum_{s=1}^{N_s} \pi_s P_{t,s}^{\text{ex},k} - P_{t,\text{iter}-1}^{\text{ex},k} \right| \right) \quad (33)$$

subject to

$$\begin{aligned} P_{t,s}^{\text{im},k} + P_{t,s}^{\text{MT}} + P_{t,s}^{\text{W}} + P_{t,s}^{\text{PV}} - P_{t,s}^{\text{ex},k} - P_{t,s}^{\text{SL}} \\ - \sum_{\omega} (P_{\omega,t,s}^{\text{in,PL}} - P_{\omega,t,s}^{\text{out,PL}}) u_{\omega}^{\text{PL}} \\ - \sum_{\omega} \sum_{b=1}^{N_b} (P_{\omega,t,s}^{c,b} - P_{\omega,t,s}^{d,b}) u_{\omega}^{\text{BESS}} = 0 \lambda_{t,s}^1 \end{aligned} \quad (34)$$

$$\begin{aligned} \underline{P} \leq \sum_{\omega} (P_{\omega,t,s}^{\text{in,PL}} - P_{\omega,t,s}^{\text{out,PL}}) u_{\omega}^{\text{PL}} \\ - \sum_{\omega} \sum_{b=1}^{N_b} (P_{\omega,t,s}^{c,b} - P_{\omega,t,s}^{d,b}) u_{\omega}^{\text{BESS}} \leq \overline{P} \lambda_{t,s}^2, \lambda_{t,s}^3 \end{aligned} \quad (35)$$

$$\begin{aligned} P_{t,\max}^{\text{W}} - P_{t,s}^{\text{W}} - P_{t,\max}^{\text{PV}} - P_{t,s}^{\text{PV}} - S_{t,s}^{\text{do,MT}} - P_{t,s}^{\text{cur}} \\ - \sum_{\omega} \sum_{b=1}^{N_b} S_{\omega,t,s}^{\text{do},b} u_{\omega}^{\text{BESS}} \leq 0 \lambda_{t,s}^4 \end{aligned} \quad (36)$$

$$P_{t,s}^W - P_{t,\min}^W + P_{t,s}^{PV} - P_{t,\min}^{PV} - S_{t,s}^{\text{up,MT}} - \sum_{\omega} \sum_{b=1}^{N_b} S_{\omega,t,s}^{\text{up},b} u_{\omega}^{\text{BESS}} \leq 0 \lambda_{t,s}^5 \quad (37)$$

$$\sum_{\omega} u_{\omega}^{\text{PL}} = 1 \sigma_{\text{PL}} \quad (38)$$

$$\sum_{\omega} u_{\omega}^{\text{BESS}} = 1 \sigma_{\text{BESS}} \quad (39)$$

$$u_{\omega}^{\text{PL}}, u_{\omega}^{\text{BESS}} \geq 0 \quad (40)$$

in addition to constraints (13)–(22), (24), and (25).

The load balancing constraint (34), prosumers' demand limits (35), and SRs (36)–(37) represent coupling constraints. Equations (38) and (39) are convexity constraints. $\lambda_{t,s}^m$, σ_{PL} , and σ_{BESS} indicate the dual variables.

Subproblems: The master problem proposes dual variables $\lambda_{t,s}^m$, σ_{PL} , and σ_{BESS} to the PL operators and D-BESS aggregators. Based on these dual variables, PL operators and D-BESS aggregators optimize their respective subproblems to generate new proposals. The PL operators' and D-BESS aggregators' subproblems are characterized by (41) and (42), respectively

$$\min \sum_{t=1}^T \sum_{s=1}^{N_s} \left(\left(\rho_t^c \pi_s + \sum_{m=1}^3 \lambda_{t,s}^m \right) P_{t,s}^{\text{in,PL}} + \left(-\rho_t^d \pi_s - \sum_{m=1}^3 \lambda_{t,s}^m \right) P_{t,s}^{\text{out,PL}} \right) - \sigma_{\text{PL}} \quad (41)$$

subject to constraints (5)–(9)

$$\min \sum_{t=1}^T \sum_{s=1}^{N_s} \sum_{b=1}^{N_b} \left(\left(\rho_t^c \pi_s + \sum_{m=1}^3 \lambda_{t,s}^m \right) P_{t,s}^{c,b} + \left(-\rho_t^d \pi_s - \sum_{m=1}^3 \lambda_{t,s}^m \right) P_{t,s}^{d,b} + (\rho_t^{\text{do}} \pi_s + \lambda_{t,s}^4) S_{t,s}^{\text{do},b} + (\rho_t^{\text{up}} \pi_s + \lambda_{t,s}^5) S_{t,s}^{\text{up},b} \right) - \sigma_{\text{BESS}} \quad (42)$$

subject to constraints (5)–(8), (10), (26), and (27).

B. Shapley Value Method

In cooperative game theory, the SVM is a concept to fairly allocate profit/cost to all the players working in a coalition. The SVM also effectively considers the unequal contribution of each player working in a coalition. Let the total number of MGs be n , and $|S|$ be the total number of MGs in coalition S . The Shapley value, ϕ_t^k for time period t for k th MG, can be calculated as [32]

$$\phi_t^k = \sum_S \left(\frac{(n-|S|)! (|S|-1)!}{n!} \right) (\psi_t(S) - \psi_t(S - \{k\})) \quad (43)$$

where $\psi_t(S)$ is the total profit/cost of coalition S and $\psi_t(S - \{k\})$ is profit/cost of coalition S without participation of k th MG. $\psi_t(S)$ can be defined as

$$\psi_t(S) = \sum_{k \in S} \left(P_t^{\text{im},k} \rho_t^{\text{im},k} - P_t^{\text{ex},k} \rho_t^{\text{ex},k} \right)$$

$$- \left(\max \left(0, \sum_{k \in S} \left(P_t^{\text{im},k} - P_t^{\text{ex},k} \right) \right) \rho_t^{c,\text{DU}} + \min \left(0, \sum_{k \in S} \left(P_t^{\text{im},k} - P_t^{\text{ex},k} \right) \right) \rho_t^{d,\text{DU}} \right). \quad (44)$$

C. Tariff Update

After fairly allocating the hourly profit/cost, the tariff for all MGs can be updated for the next iteration in the following manner:

$$\rho_{t,\text{iter}+1}^{\text{im},k} = \begin{cases} \frac{P_t^{\text{im},k} \rho_t^{\text{im},k} - \phi_t^k}{P_t^{\text{im},k}}, & \text{if } P_t^{\text{im},k} \neq 0 \\ \rho_t^{\text{im},k}, & \text{otherwise} \end{cases} \quad (45)$$

$$\rho_{t,\text{iter}+1}^{\text{ex},k} = \begin{cases} \frac{P_t^{\text{ex},k} \rho_t^{\text{ex},k} + \phi_t^k}{P_t^{\text{ex},k}}, & \text{if } P_t^{\text{ex},k} \neq 0 \\ \rho_t^{\text{ex},k}, & \text{otherwise.} \end{cases} \quad (46)$$

Based on the updated tariff for MGs by MGA, the MGO updates tariff of its prosumers and consumers. The updated tariff for prosumers and consumers can be written as

$$\rho_{t,\text{iter}+1}^c = \begin{cases} 1.1 \rho_{t,\text{iter}+1}^{\text{im},k}, & \text{if } P_t^{\text{im},k} \neq 0 \\ 1.1 \rho_{t,\text{iter}+1}^{\text{ex},k}, & \text{if } P_t^{\text{ex},k} \neq 0 \\ \rho_t^c, & \text{otherwise} \end{cases} \quad (47)$$

$$\rho_{t,\text{iter}+1}^d = \begin{cases} 0.9 \rho_{t,\text{iter}+1}^{\text{im},k}, & \text{if } P_t^{\text{im},k} \neq 0 \\ 0.9 \rho_{t,\text{iter}+1}^{\text{ex},k}, & \text{if } P_t^{\text{ex},k} \neq 0 \\ \rho_t^d, & \text{otherwise.} \end{cases} \quad (48)$$

The energy management framework¹ used in this article is depicted in Fig. 3. MGOs perform a decentralized energy management optimization parallelly to meet consumer demand after collecting data at the first level. The SDWD method is used for decentralized energy management optimization. SDWD converges to the optimal point by iterating between the master problem and the subproblems of PLs and D-BESSs. The master problem contains the MG's constraints (13)–(22), (24), (25) and all coupling constraints (34)–(37). MGO solves the master problem (30) and proposes the optimal dual variables vectors associated with coupling constraints (34)–(37) and convexity constraints (38)–(39) to the PL operator and D-BESS aggregator subproblems. The PL operator and D-BESS aggregator use these dual variables to solve their respective subproblems and propose the new proposals to the master problem. This process of exchanging dual variables vectors and proposals continues until the convergence of SDWD. Followed by this optimization, all MGOs send their energy requests to MGA. After that, MGA update tariffs according to MGOs' power exchange requests as given in (45)–(46). For rescheduling, MGOs determine the tariffs (47)–(48) for their prosumers and consumers after receiving MGA's new tariffs. This process is repeated until the stopping criterion is reached.

The DWD method always converges to the original problem's optimal solution. The solution path of the master problem with

¹Approximate bandwidth required to meet the communication requirement of the proposed method with a single PL operator and D-BESS aggregator is approximately 4 (uplink) and 2 Mb/s (downlink) for 20-ms latency. Existing 4G communication technologies are sufficient to meet the communication requirement for the proposed algorithm.

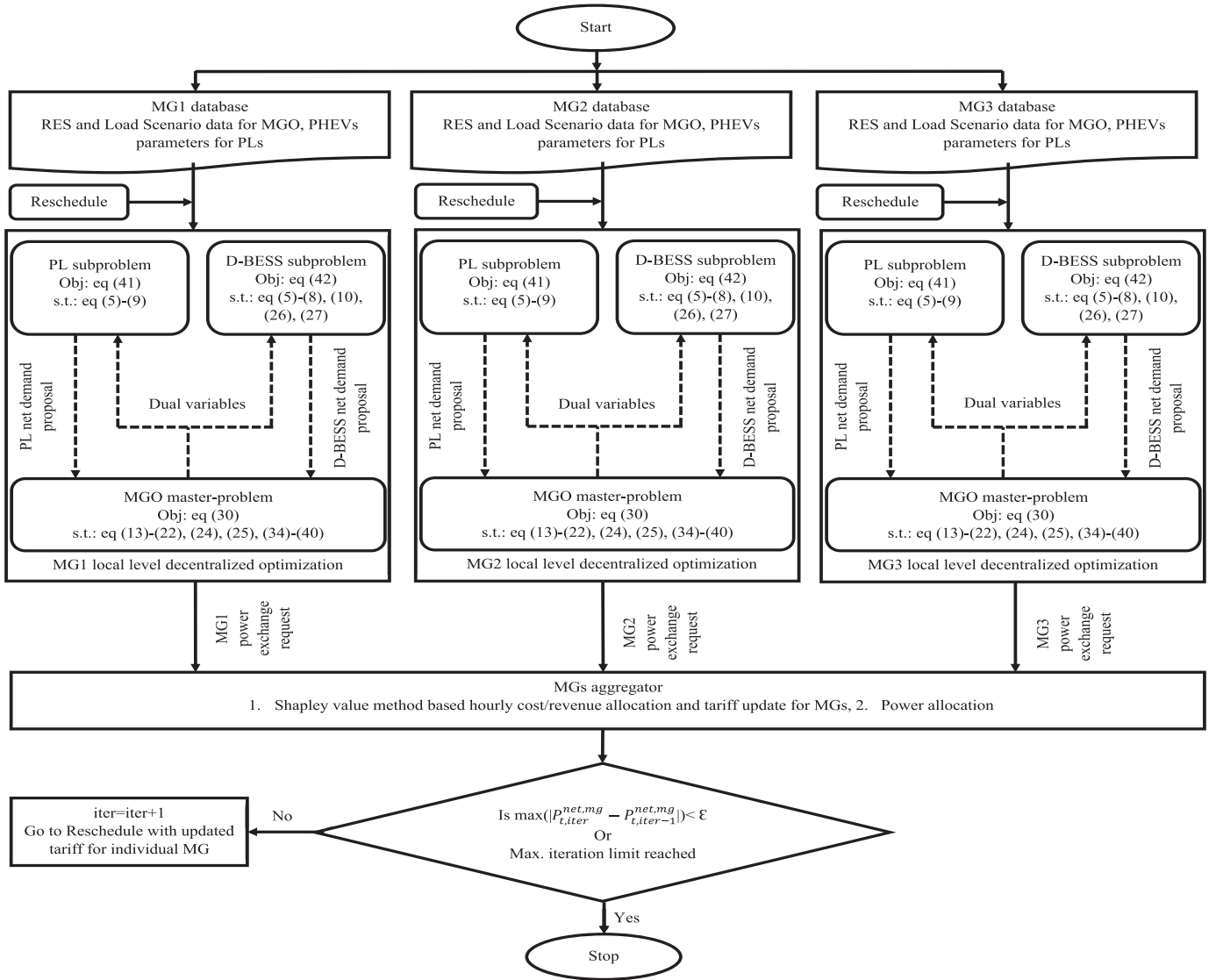


Fig. 3. Energy management framework flow diagram.

a more complex feasible region may be longer than the original problem. For \bar{n} -dimensional vector of decision variables and \bar{m} master problem constraints (excluding convexity constraints), the complexity of an iteration in the DWD method is $\mathcal{O}(\bar{n}\bar{m})$. In actual practice, a compromise needs to be made between the optimal gap and the computation time. The exponential time complexity of the SVM and the computational complexity of the SDWD method are the main issues in the proposed algorithm.

V. SIMULATION RESULTS

In this article, three MGs with different load profiles and generation capacities are considered. The predicted conventional elastic loads of MGs are depicted in Fig. 4. The assumed load elasticity coefficients are given in Table I. The wind power ratings are 3 MW each for MG1 and MG3, and 3.5 MW for MG2. The PV rating is 1.5 MW for all the MGs. The rated capacities of MTs are 1.8 MW for MG1 and 1.5 MW for MG2

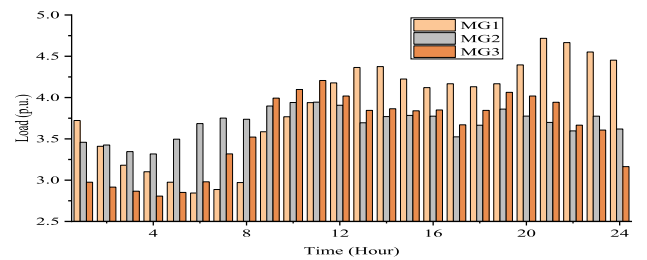


Fig. 4. Load profile of MGs.

TABLE I
ELASTICITY COEFFICIENTS

	Peak Period	Shoulder Period	Valley Period
Peak Period	-0.2	0.016	0.012
Shoulder Period	0.008	-0.2	0.01
Valley Period	0.006	0.008	-0.2

TABLE II
DU'S ELECTRICITY TARIFF

Hour	1	2	3	4	5	6	7	8	9	10	11	12
$\rho_t^{DU}, \text{€}/\text{kWh}$	0.071	0.063	0.058	0.053	0.054	0.061	0.071	0.085	0.087	0.095	0.105	0.113
Hour	13	14	15	16	17	18	19	20	21	22	23	24
$\rho_t^{DU}, \text{€}/\text{kWh}$	0.112	0.120	0.132	0.144	0.150	0.146	0.142	0.126	0.129	0.127	0.114	0.093

and MG3. The rated battery capacities are assumed to be 80 kW for D-BESSs and 15.6–27.6 kW for PHEVs [33]. The maximum charging and discharging rates are 40 kW/h for D-BESS. The charging and discharging efficiencies are assumed to be 95%. The day-ahead DU's electricity tariff is given in Table II. The feed-in tariff is considered as half of the electricity tariff. The emission rate is assumed to be 0.01695 € /kWh. The proposed framework has been implemented on a system with a Core i3 1.20 GHz processor and 4-GB RAM. The GAMS/CPLEX solver is used for solving the optimization problem.

Three different cases are considered to demonstrate the effectiveness of the proposed EMS as follows.

Case I (Base Case): In this case, each MG optimizes its objective function, and there is no cooperation among MGs. All MGs exchange their power with DU only.

Case II: In this case, the MGA acts as an intermediate among MGs and DU. The MGA receives power exchange requests from all MGs. Based on the power exchange requests, MGA allocates power and updates tariffs for MGs according to Shapley values.

In *Case I* and *Cases II*, each MG uses the updated tariff given in (47) and (48) for its prosumers and consumers.

Case III: This case is used for comparative analysis of proposed EMS with the existing state of art. In this case, the tariff for MGs' prosumers and consumers is based on DU's electricity tariff rather than the updated price given in (47) and (48). ρ_t^c and ρ_t^d are assumed to be $1.1\rho_t^{c,DU}$ and $0.9\rho_t^{d,DU}$, respectively. This case has the following considerations.

Case III(a): There is no power trading among MGs.

Case III(b): This case is similar to *Case II* except for tariff updates for MGs' prosumers and consumers.

Case III(c): In this case, the Nash bargaining theory-based incentive mechanism [23] is used for scheduling. The power exchange requests of MGs are depicted in Fig. 5(a) and (b) for *Case I* and *Case II*, respectively. It can be seen that the MGs' scheduled power exchange increases in *Case II* as compared with *Case I*, i.e., MG3 requests for more power import during 11:00 to 13:00 h and during the same time interval, MG1 and MG2 increase their power export. The reason behind this change is the updated tariff for MGs due to cooperative scheduling and Shapley value allocation. The tariffs for MGs are represented in Fig. 6. As shown in the figure, the MG1 and MG2 are able to sell their power at a higher rate in *Case II* compared with DU's feed-in tariff in *Case I*. Similarly, MG3 can purchase power at a lower rate as compared with DU's energy tariff at the same instant.

The dotted line in Fig. 6 indicates the DU's energy tariff, whereas the solid line represents the DU's feed-in tariff. Fig. 6(a) depicts that MGs' tariff is always equal to DU's energy selling/feed-in price when the MG imports/exports power, irrespective of other MGs' power, exchange scenarios. In *Case II*, the tariff for MG also depends on other MGs' circumstances. If some MGs in a coalition are willing to import the power and

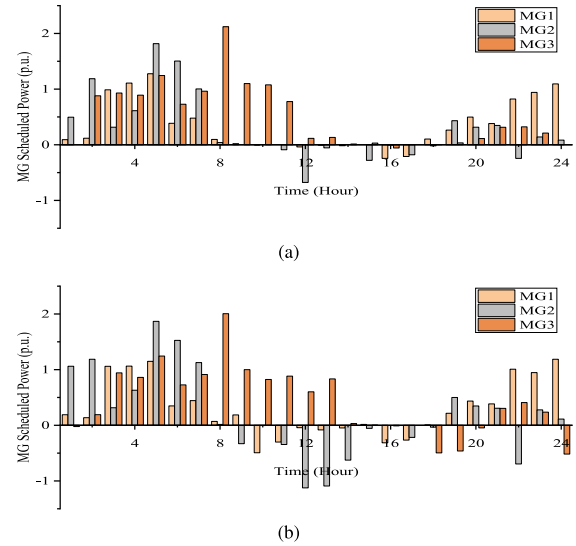


Fig. 5. Scheduled power exchange of MGs. (a) *Case I*. (b) *Case II*.

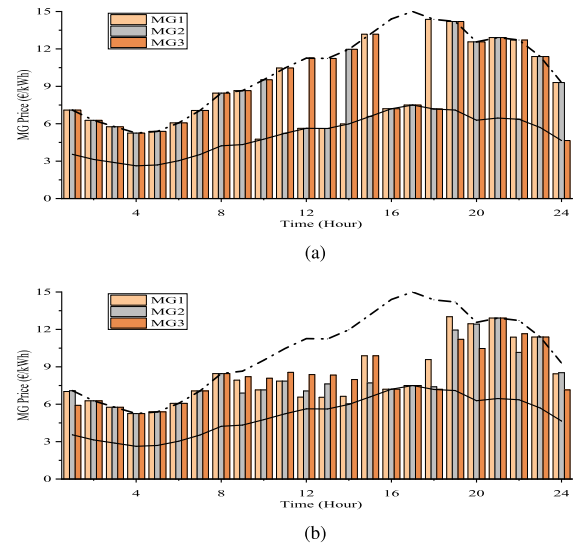
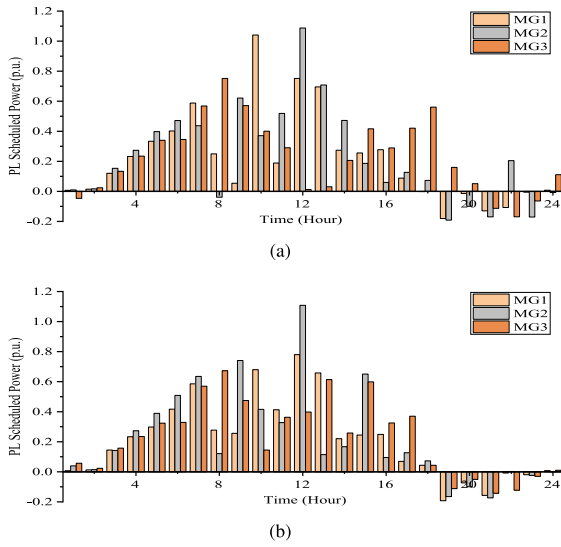
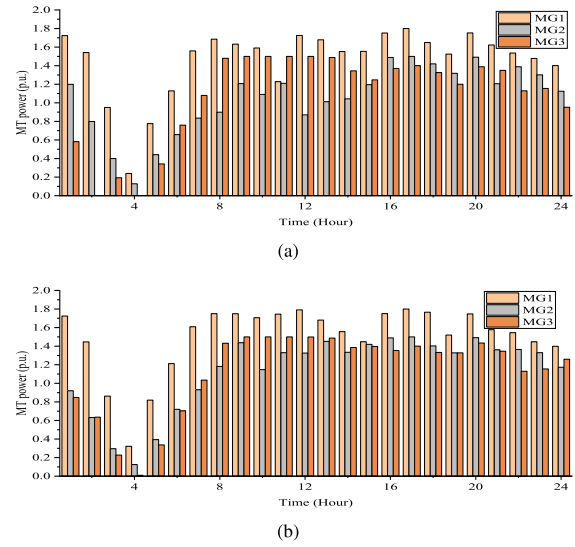
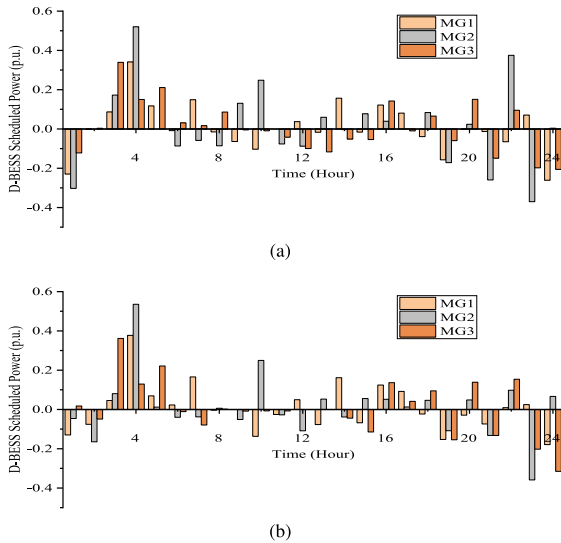
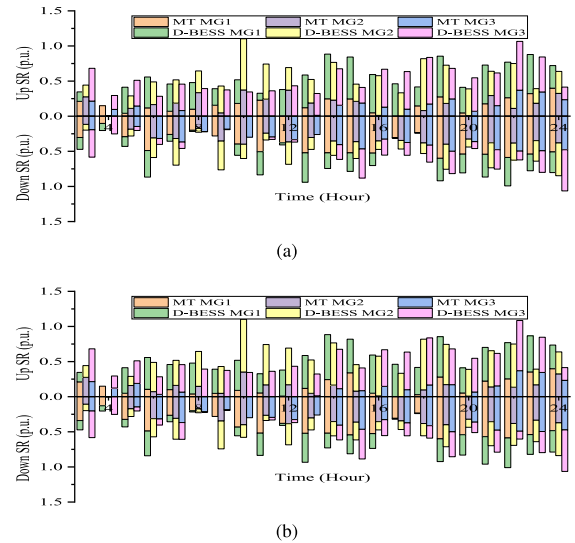


Fig. 6. Power exchange tariff for MGs. (a) *Case I*. (b) *Case II*.

others consent to export power, they can be settled on a price between DU's selling price and feed-in tariff. For example, in *Case II*, Fig. 6(b), during 9:00 to 15:00, 18:00 to 20:00, and 22:00 to 24:00 h, the energy prices are below DU's selling price but higher than the DU's feed-in tariff. This situation is advantageous for all participants in the coalition as they can reduce their power import cost or increase their power export price. Therefore, the proposed pricing mechanism ensures that the energy import price for buyer MGs is always less than or

Fig. 7. Scheduled power of PLs. (a) *Case I*. (b) *Case II*.Fig. 9. MT scheduled power. (a) *Case I*. (b) *Case II*.Fig. 8. Scheduled power of D-BESS. (a) *Case I*. (b) *Case II*.Fig. 10. D-BESS and MT contribution in SRs. (a) *Case I*. (b) *Case II*.

equal to DU's energy tariff. The energy export price for seller MGs is always greater than or equal to DU's feed-in tariff. The tariff for an MG depends on two factors; the contribution of MG in the energy pool as a seller/buyer and the deficit/surplus amount of energy of other MGs.

According to its power import/export tariff, the MGO updates its charging/discharging tariff for prosumers and consumers of its entity. Thus, as shown in Figs. 7 and 8, the scheduled power demands of PLs and D-BESSs are also changed according to the tariff received by MGO. The power demand of PL in MG1 has a peak point at 10:00 h in *Case I* because of the low tariff at this time interval compared to neighboring time intervals. But the PL demand is distributed from 9:00 to 11:00 h in *Case II*, as the tariff of MG1 increases at 10:00 h and decreases at 9:00 and 11:00 h. Similarly, all PLs and D-BESSs change their power demands according to change in tariffs.

The power outputs of scheduled MTs are shown in Fig. 9. The higher power export tariff encourages more power generation from MTs. MG1 and MG2 increase their generation during the mid-day period, where they export power, whereas MG3 imports power. MG3 raise its generation at 24:00 h to export power to MG1 and MG2. Besides the power export tariff, MT generation depends on its ramp rate constraints and other system conditions. There is no change in tariff in both the cases and there is a negligible difference between MG3 tariff and MT generation cost at 2:00 h, so MT in MG3 generates more power to satisfy the demand and ramp rate constraints.

The contribution of D-BESSs and MT in up/down-SR to cope with the uncertainties due to RES are shown in Fig. 10. In both the cases, the SR requirements are approximately the same. But the contribution of D-BESS and MT are different, as the scheduled powers are subjected to energy tariff. The expected

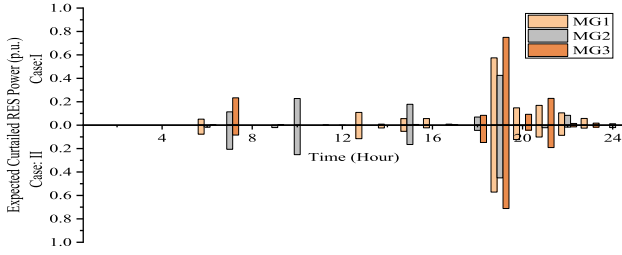


Fig. 11. Expected RES power curtailment.

TABLE III
COST COMPARISON FOR DIFFERENT CASES

		Case I	Case II
MG operating Cost (€)	MG1	3640.618	3584.588
	MG2	2905.860	2835.171
	MG3	3398.049	3319.453
PLs' Cost (€)	MG1	343.633	379.376
	MG2	368.925	399.365
	MG3	507.545	460.172
D-BESSs' Cost (€)	MG1	-376.103	-386.845
	MG2	-389.785	-407.258
	MG3	-380.731	-388.249
F (€)	MG1	3997.206	3976.016
	MG2	3280.124	3251.381
	MG3	3917.076	3793.984
Avg power import price (€/kWh)	MG1	0.092	0.087
	MG2	0.086	0.083
	MG3	0.094	0.082
Avg power export price (€/kWh)	MG1	0.061	0.071
	MG2	0.067	0.075
	MG3	0.071	0.082

RES power curtailment to contribute in down-SR is shown in Fig. 11. If MT and D-BESS are not sufficient to fulfill the down-SR, RES power to be curtailed with high curtailment charges. The outcomes of both the cases are summarized in Table III. In *Case II*, the operation cost, which includes MT generation cost, power exchange cost, and SR cost, reduces from 3640.618 to 3584.588 €/day for MG1, 2905.860 to 2835.171 €/day for MG2, and 3398.049 to 3319.453 €/day for MG3. However, the cost of PLs increases from 343.633 to 379.376 €/day in MG1 and 368.925 to 399.365 €/day in MG2, whereas it reduces from 507.545 to 460.172 €/day in MG3. As stated earlier, MGOs provide tariffs to their prosumers and consumers based on the tariffs they receive from MGA. The PLs and D-BESSs optimize their scheduling according to these tariffs. The MG1 and MG2 get higher tariffs when they export power during 8:00 to 14:00 h in *Case II* compared to *Case I*. Most of the charging in PLs occurs during these hours due to the restriction of PHEVs' parking time slots, as shown in Fig. 2(a). So, the PL operators in MG1 and MG2 have to pay higher amount for energy purchase in *Case II*. But MG3 imports energy during this duration at a lower rate as compared to *Case I*. So, the PL cost in MG3 reduces in *Case II*. The D-BESS aggregator profit increases in *Case II*, as depicted in Table III. D-BESSs have greater flexibility to shift their scheduling than PLs because they are not constrained by arrival and departure times. The overall energy cost F reduce from 3997.206 to 3976.016 €/day, 3280.124 to 3251.381 €/day, and 3917.076 to 3793.984 €/day for MG1, MG2, and MG3,

TABLE IV
COST COMPARISON FOR CASE III

		Case III(a)	Case III(b)	Case III(c)
MG operating Cost (€)	MG1	3680.374	3651.316	3665.588
	MG2	2974.824	2928.177	2959.833
	MG3	3444.901	3378.979	3430.107
PLs' Cost (€)	MG1	514.308	504.745	499.521
	MG2	532.233	528.48	517.242
	MG3	563.601	551.722	548.808
D-BESSs' Cost (€)	MG1	-374.191	-384.372	-388.977
	MG2	-397.859	-407.354	-412.851
	MG3	-359.793	-369.949	-374.587
F (€)	MG1	4229.259	4186.263	4171.888
	MG2	3532.070	3473.867	3474.699
	MG3	4051.723	3958.735	3994.354

respectively. The average power import price for all the three MGs decreases by 5.368%, 2.844%, and 13.07%, whereas the average power export price for all MGs increases by 15.51%, 13.12%, and 13.85% in *Case II* as compared with *Case I*.

The net demand of all the three MGs for *Case III* is shown in Fig. 12. MGs exchange more power in *Case III(b)* and *Case III(c)* as compared with *Case III(a)*. However, both mechanisms used in *Case III(b)* and *Case III(c)* encourage MGs to trade power among themselves. But the net demands of MGs are not exactly the same in *Case III(b)* and *Case III(c)*. The allocation of SVM-based hourly profit/cost is used to update MGs' import/export tariffs in *Case III(b)*, whereas the Nash bargaining method in *Case III(c)* is used to distribute the profit among MGs after the cooperative scheduling to reduce the energy cost functions F of all MGs. The cost comparison of *Case III* is depicted in Table IV. The MG operating cost is lower in *Case III(b)* as compared with *Case III(a)* and *Case III(c)*. The total energy cost of all MGs, i.e., the sum of energy cost functions F of all MGs are 11813.052, 11618.865, and 11640.941 €/day for *Case III(a)*, *Case III(b)*, and *Case III(c)*, respectively. So, the total energy cost of all MGs is almost same for *Case III(b)* and *Case III(c)* as compared with *Case III(a)*. Also, *Case III(b)* appears marginally better than *Case III(c)*, and the energy cost functions F of all MGs are much lower in *Case II* as compared with *Case III*. Therefore, the proposed EMS can effectively reduce energy costs.

VI. CONCLUSION

The numerical results establish the effectiveness of the proposed energy management approach to minimize the energy cost. A DWD is an efficient tool for achieving the goals of MGO, PL operators, and D-BESS aggregators in a decentralized fashion with minimal information exchange. The D-BESSs and MTs can be used as SRs to cope with the associated uncertainties in the system. The MG aggregator uses the SVM to fairly allocate the cost/revenue and update the energy tariff for MGO. The results show that hourly power import price of each MGO is less than or equal to the tariff of DU and hourly power export price of each MGO is higher than or equal to feed-in tariff of DU. This updated energy tariff at MG aggregator level prompt MGOs to exchange power among themselves rather than with DU. The cost comparison demonstrates that cooperative operation in the proposed framework yields significant reduction in the MGs' operating cost. Also, the average power import price significantly decreases while the average power export

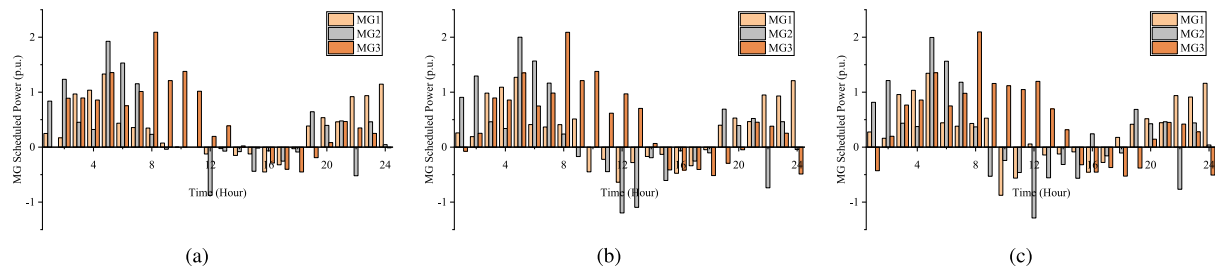


Fig. 12. MGs scheduled power. (a) Case III(a). (b) Case III(b). (c) Case III(c).

price increases in a cooperative approach. Thus, the proposed technique is beneficial in terms of cost savings as well as less dependence on DU. Further research intends to incorporate the SR sharing among MGOs and role of DNO in networked MMG energy management.

REFERENCES

- [1] K. Mahmud, M. J. Hossain, and G. E. Town, "Peak-load reduction by coordinated response of photovoltaics, battery storage, and electric vehicles," *IEEE Access*, vol. 6, pp. 29353–29365, 2018.
- [2] Q. Kang, S. Feng, M. Zhou, A. C. Ammari, and K. Sedraoui, "Optimal load scheduling of plug-in hybrid electric vehicles via weight-aggregation multi-objective evolutionary algorithms," *IEEE Trans. Intell. Transp. Syst.*, vol. 18, no. 9, pp. 2557–2568, Sep. 2017.
- [3] E. Veldman and R. A. Verzijlbergh, "Distribution grid impacts of smart electric vehicle charging from different perspectives," *IEEE Trans. Smart Grid*, vol. 6, no. 1, pp. 333–342, Jan. 2015.
- [4] H. Fathabadi, "Utilization of electric vehicles and renewable energy sources used as distributed generators for improving characteristics of electric power distribution systems," *Energy*, vol. 90, pp. 1100–1110, 2015.
- [5] Y. Zheng, K. Meng, F. Luo, J. Qiu, and J. Zhao, "Optimal integration of MBESSs/SBESSs in distribution systems with renewables," *IET Renewable Power Gener.*, vol. 12, no. 10, pp. 1172–1179, 2018.
- [6] C. Hutson, G. K. Venayagamoorthy, and K. A. Corzine, "Intelligent scheduling of hybrid and electric vehicle storage capacity in a parking lot for profit maximization in grid power transactions," in *Proc. IEEE Energy 2030 Conf.*, 2008, pp. 1–8.
- [7] M. Shafie-Khah, P. Siano, D. Z. Fitriwi, N. Mahmoudi, and J. P. Catalao, "An innovative two-level model for electric vehicle parking lots in distribution systems with renewable energy," *IEEE Trans. Smart Grid*, vol. 9, no. 2, pp. 1506–1520, Mar. 2018.
- [8] İ. Şengör, O. Erdiñç, B. Yener, A. Taşçıkaraoğlu, and J. P. Catalão, "Optimal energy management of EV parking lots under peak load reduction based DR programs considering uncertainty," *IEEE Trans. Sustain. Energy*, vol. 10, no. 3, pp. 1034–1043, Jul. 2019.
- [9] M. J. E. Alam, K. M. Muttaqi, and D. Sutanto, "A controllable local peak-shaving strategy for effective utilization of PEV battery capacity for distribution network support," *IEEE Trans. Ind. Appl.*, vol. 51, no. 3, pp. 2030–2037, May/Jun. 2015.
- [10] L. Liu, F. Kong, X. Liu, Y. Peng, and Q. Wang, "A review on electric vehicles interacting with renewable energy in smart grid," *Renewable Sustain. Energy Rev.*, vol. 51, pp. 648–661, 2015.
- [11] C. Shao, X. Wang, X. Wang, C. Du, C. Dang, and S. Liu, "Cooperative dispatch of wind generation and electric vehicles with battery storage capacity constraints in SCUC," *IEEE Trans. Smart Grid*, vol. 5, no. 5, pp. 2219–2226, Sep. 2014.
- [12] L. Cheng, Y. Chang, and R. Huang, "Mitigating voltage problem in distribution system with distributed solar generation using electric vehicles," *IEEE Trans. Sustain. Energy*, vol. 6, no. 4, pp. 1475–1484, Oct. 2015.
- [13] A. M. Jadhav and N. R. Patne, "Priority-based energy scheduling in a smart distributed network with multiple microgrids," *IEEE Trans. Ind. Informat.*, vol. 13, no. 6, pp. 3134–3143, Dec. 2017.
- [14] Z. Wang, B. Chen, J. Wang, and J. Kim, "Decentralized energy management system for networked microgrids in grid-connected and islanded modes," *IEEE Trans. Smart Grid*, vol. 7, no. 2, pp. 1097–1105, Mar. 2016.
- [15] M. R. Sandgani and S. Sirouspour, "Priority-based microgrid energy management in a network environment," *IEEE Trans. Sustain. Energy*, vol. 9, no. 2, pp. 980–990, Apr. 2018.
- [16] Y. Wang, S. Mao, and R. M. Nelms, "On hierarchical power scheduling for the macrogrid and cooperative microgrids," *IEEE Trans. Ind. Informat.*, vol. 11, no. 6, pp. 1574–1584, Dec. 2015.
- [17] N. Nikmehr and S. Najafi-Ravadanegh, "Optimal operation of distributed generations in micro-grids under uncertainties in load and renewable power generation using heuristic algorithm," *IET Renewable Power Gener.*, vol. 9, no. 8, pp. 982–990, 2015.
- [18] A. Parisio, C. Wiezorek, T. Kyntäjää, J. Elo, K. Strunz, and K. H. Johansson, "Cooperative MPC-based energy management for networked microgrids," *IEEE Trans. Smart Grid*, vol. 8, no. 6, pp. 3066–3074, Nov. 2017.
- [19] S. A. Arefifar, M. Ordonez, and Y. A. -R. I. Mohamed, "Energy management in multi-microgrid systems-development and assessment," *IEEE Trans. Power Syst.*, vol. 32, no. 2, pp. 910–922, Mar. 2017.
- [20] Y. Du *et al.*, "A cooperative game approach for coordinating multi-microgrid operation within distribution systems," *Appl. Energy*, vol. 222, pp. 383–395, 2018.
- [21] H. Karimi and S. Jadid, "Optimal energy management for multi-microgrid considering demand response programs: A stochastic multi-objective framework," *Energy*, vol. 195, 2020, Art. no. 116992.
- [22] S. E. Ahmadi and N. Rezaei, "A new isolated renewable based multi microgrid optimal energy management system considering uncertainty and demand response," *Int. J. Elect. Power Energy Syst.*, vol. 118, 2020, Art. no. 105760.
- [23] H. Wang and J. Huang, "Incentivizing energy trading for interconnected microgrids," *IEEE Trans. Smart Grid*, vol. 9, no. 4, pp. 2647–2657, Jul. 2018.
- [24] X. Liu, B. Gao, Z. Zhu, and Y. Tang, "Non-cooperative and cooperative optimisation of battery energy storage system for energy management in multi-microgrid," *IET Gener., Transmiss., Distrib.*, vol. 12, no. 10, pp. 2369–2377, 2018.
- [25] J. Zhang *et al.*, "A bi-level program for the planning of an islanded microgrid including CAES," *IEEE Trans. Ind. Appl.*, vol. 52, no. 4, pp. 2768–2777, Jul./Aug. 2016.
- [26] "U. S. Department of Transportation, Federal Highway Administration, 2017 National Household Travel Survey (n.d)," Jan. 2020. [Online]. Available: <https://nhts.orl.gov>
- [27] A. Lojowska, D. Kurowicka, G. Papaefthymiou, and L. van der Sluis, "Stochastic modeling of power demand due to EVs using copula," *IEEE Trans. Power Syst.*, vol. 27, no. 4, pp. 1960–1968, Nov. 2012.
- [28] N. Growe-Kuska, H. Heitsch, and W. Romisch, "Scenario reduction and scenario tree construction for power management problems," in *Proc. IEEE Bologna Power Tech Conf. Proc.*, vol. 3, 2003, p. 7.
- [29] M. Carrión and J. M. Arroyo, "A computationally efficient mixed-integer linear formulation for the thermal unit commitment problem," *IEEE Trans. Power Syst.*, vol. 21, no. 3, pp. 1371–1378, Aug. 2006.
- [30] F. C. Schweppe, M. C. Caramanis, R. D. Tabors, and R. E. Bohn, *Spot Pricing of Electricity*. Boston, MA, USA: Springer, 1988.
- [31] A. J. Conejo, E. Castillo, R. Minguez, and R. Garcia-Bertrand, *Decomposition Techniques in Mathematical Programming: Engineering and Science Applications*. Berlin, Germany: Springer, 2006.
- [32] A. E. Roth, *The Shapley Value: Essays in Honor of Lloyd S. Shapley*. Cambridge, U.K.: Cambridge Univ. Press, 1988.
- [33] S. Shafiee, M. Fotuhi-Firuzabad, and M. Rastegar, "Investigating the impacts of plug-in hybrid electric vehicles on power distribution systems," *IEEE Trans. Smart Grid*, vol. 4, no. 3, pp. 1351–1360, Sep. 2013.